Theoretical and experimental researches on a PCF-based SPR sensor*

BING Pi-bin(邴丕彬)[1**], **LI Zhong-yang**(李忠洋)[1], **YAO Jian-quan**(姚建铨)[2], **LU Ying**(陆颖)[2], **DI Zhi-gang** (邸志刚)[2], **and YAN Xin**(闫昕)[3]

1. *Institute of Electric Power, North China University of Water Resources and Electric Power, Zhengzhou 450011, China*
2. *Key Laboratory of Optoelectronic Information Technology, Ministry of Education, Institute of Laser and Optoelectronics, College of Precision Instrument and Optoelectronics Engineering, Tianjin University, Tianjin 300072, China*
3. *College of Optronics Engineering, Zaozhuang University, Zaozhuang 277160, China*

(Received 13 February 2012)

A photonic crystal fiber based surface plasmon resonance (PCF-SPR) sensor is simulated by finite element method and experimentally realized. The calculations show that there is an obvious loss peak in the vicinity of 1.2 μm while the PCF of LMA-8 is used as a sensor. The suspension of silver nanoparticle mixed with hexadecyl trimethyl ammonium bromide (CTAB) is inhaled into the PCF to form a metal film which can be stimulated to generate plasmon in the experiment. A spectrometer is utilized to detect the continuous broadband transmission spectrum from the PCF. The experimental results verify the loss peak. Compared with the theoretical calculations, the offset of loss peak about 40 nm can be acceptable, because the uniformity of the metal coating is difficult to guarantee and the film thickness is difficult to control.

Document code: A **Article ID:** 1673-1905(2012)04-0245-4
DOI 10.1007/s11801-012-1182-4

Surface plasmon is extremely sensitive to the variation of the surrounding dielectric medium while it propagates at the metal-dielectric interface, so surface plasmon resonance (SPR) has been widely implemented in sensing fields[1]. Especially, optical fiber based SPR sensor has important applications in chemical, biological, medical researches, etc[2-5]. Recently, a new type of photonic crystal fiber (PCF) provided a guideline for the new sensors. The design of PCF is flexible, because the transmission of light could be controlled by changing the array of the air-holes. A. Hassani and M. Skorobogatiy[6,7] firstly introduced the concept of PCF-SPR sensor. They analyzed the design principles of two different PCF structures with gold coating for biosensing applications in detail. But most researches on the PCF-SPR sensor are still on theoretical stage so far, because there are difficulties on manufacturing designed PCF, coating metal nanofilm, microfluidic infiltration in micro core hole of PCF, achieving continuous broadband coherent light source, and so on.

In this paper, the PCF-SPR sensor with metal coating is theoretically simulated and experimentally realized. We conduct experiments with PCF of LMA-8 produced by the NKT Photonics. A bromine tungsten lamp is selected as the light source, and the continuous broadband fiber-coupled output can be achieved. A spectrometer is used for detecting the continuous broadband spectrum of light.

A field emission scanning electron microscopy (SEM) of S-4800 produced by Hitachi Ltd. is used, and the cross section of LMA-8 is shown in Fig.1. The cladding consists of seven layers of air-holes, and the air-holes in the seventh layer are incomplete and can be seen as the supplement of the sixth one. The pitch of the underlying hexagonal lattice is Λ = 5.6

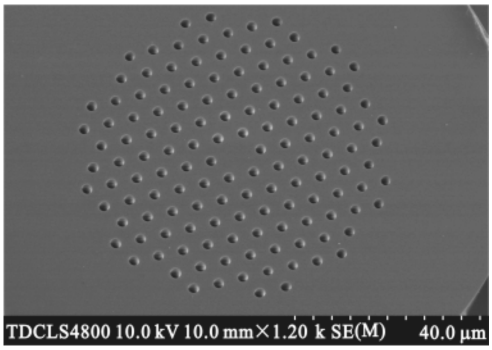

Fig.1 SEM image of LMA-8

* This work has been supported by the Major State Basic Research Development Program of China (No.2010CB327801), the Science and Technology Project of Shandong College (No.J11LG74), and the Science and Technology Project of Zaozhuang in Shandong Province (No.201127).

** E-mail: bing463233@163.com

μm, the diameter of the cladding air-holes is d = 2.576 μm, the cladding diameter is 125 μm, and the core diameter is about 8.5 μm.

Obviously, LMA-8 has a standard outer diameter of 125 μm which is compatible with all common fiber tools, so the PCF is available with hermetically sealed ends and FC/PC connectors.

A typical measured spectral attenuation of LMA-8 is shown in Fig.2. We can see that LMA-8 is optimized to exhibit the low loss in the widest possible range from 600 nm to above 1600 nm. So LMA-8 is suitable for the transmission of the broadband light in a large range.

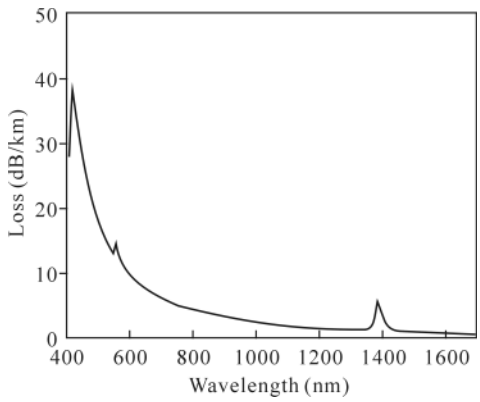

Fig.2 Typical measured spectral attenuation of LMA-8

As a PCF-SPR sensor, the most crucial requirement is the phase matching between the plasmon mode and the core-guided mode. The effective refractive index of the plasmon mode is mainly determined by the adjacent analyte, the coating metal and so on. We know that aqueous solution ($n_a \approx 1.33$) is the most common analyte. On the other hand, SPR involves the resonant excitation of plasmon or electromagnetic waves coupled with collective oscillations of free electrons in metal. So the choice of the metal medium is extremely important. Gold and silver are the most commonly used SPR metal films in the visible range[8,9]. Gold is widely used as the coating material for its excellent stable characteristics. The dielectric constant of gold is given by the Drude model which gives a good fitting to the measurement results in Ref.[10]. Although the silver film is less stable, it is also widely used as SPR metal film due to its high reflectivity and measurement sensitivity. Unfortunately, the existing models can not accurately describe the dielectric constant of silver[8,9,11], so we select the experimental results of Palik[12] as the refractive index of silver in simulation. The effective refractive index of a core-guided mode is close to that of a core material. Usually, the background material of fiber is assumed to be silica glass ($n_c \approx 1.45$). Accurately, the refractive index of the fiber is given by the Sellmeier dispersion relation[13]. In this paper, the complex propagation constants of electromagnetic mode of the sensor are investigated numerically by a full vector finite element method (FEM) with perfectly matched layer (PML) boundaries. It can be assumed that the metal film in PCF is uniform, and all the air-holes are coated. In order to simplify the calculation, the holes shown as channels for analyte infiltration are coated with 100 nm-thick layer of metal.

In Fig.3, we present the effective refractive indices of a core-guided mode of LMA-8 with and without metal coating. An overall decrease in the effective refractive indices of a core-guided mode is observed for coating silver or gold with lower refractive index. The curve of effective refractive index of a core-guided mode coated with gold is smoother than that coated with silver. The fact is easy to rationalize by noting that the refractive index of gold is idealized, and that of silver is undulating, which is obtained from experiments. Both of the curves have a significant undulance in the vicinity of 1.2 μm. That means the phase matching between the plasmon mode and core-guided mode occurs, and the surface plasmon is strongly stimulated at the metal-dielectric interface.

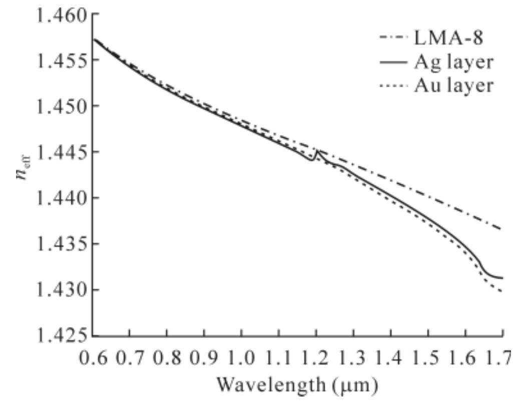

Fig.3 Dispersion characteristics of a core-guided mode of LMA-8 with and without metal coating

Dramatically, most energy transmits in the core area of the PCF, a part of the energy penetrates into the metal to excite the plasmon mode, and the energy of the core-guided mode is dissipated. It is assumed that the most loss of the core-guided mode is due to the excitation of the plasmon mode. We need to calculate the loss of the core-guided mode to determine the intensity of the excited plasmon mode. The loss of the core-guided mode, which is in proportion to the imaginary part of the effective refractive index (Im (n_{eff})), can be defined as:

$$\alpha(\text{dB/m}) = 40\,\pi \text{Im}(n_{eff})/(\ln(10\lambda)) \,, \quad (1)$$

where λ is in meters.

In Fig.4, we show the changes in the loss spectra of the plasmon peaks when LMA-8 is coated with different metals. Generally, modal propagation loss is similar when the PCFs are coated with silver or gold, and simultaneously, both of the loss spectra have a strong resonance peak in the vicinity of 1.2 μm, which are consistent with that in Fig.3. It can be concluded that LMA-8 is suitable for sensing after being coated with silver or gold. On the other hand, it can be noticed that the PCF coated with silver has another two obvious resonance peaks in the vicinity of 1.28 μm and 1.65 μm, which is because the silver has intrinsic absorption at the two wavelengths[12].

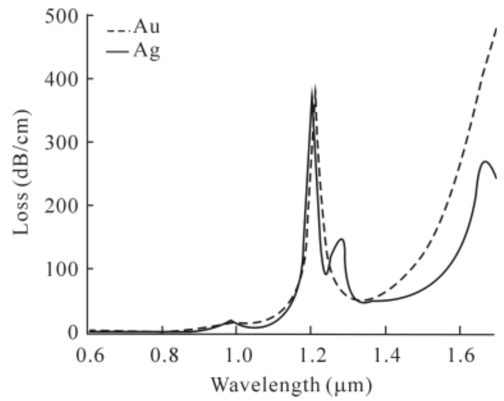

Fig.4 Loss spectra of a core-guided mode of LMA-8 coated with silver and gold, respectively

The schematic diagram of the experimental setup is shown in Fig.5. A bromine tungsten lamp of LSH-T150 can supply an ideal continuous broadband light during 250−2700 nm. The tungsten lamp regarded as a point source has a strong divergence, so a back reflector is used to improve the efficiency of the energy. A convex lens with a focal length of 150 mm is used to couple the broadband light into the SMA905 multimode fiber. The multimode fiber is connected with LMA-8 by a fiber connector.

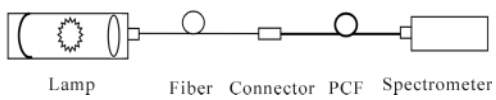

Fig.5 Schematic diagram of PCF-SPR sensor experimental system

All air-holes of LMA-8 are coated with silver in the experiment. The silver film is deposited by inhaling freshly prepared Ag solution into the array holes in PCF with a vacuum pump under the lower pressure. It is well known that $Ag(NH_3)^+$-glucose mixed solution used for silver mirror reaction is not stable, so we directly select the suspension of silver nanoparticle to penetrate into the PCF. The diameter of the silver nanoparticle is 20 nm. Because the PCF-SPR sensor needs no sample purification, the surfactant of hexadecyl trimethyl ammonium bromide (CTAB) can be mixed into the suspension of silver nanoparticle, so the suspension is stable and can be placed for a long time without precipitation. The method can be used for inhaling the particle of silver for a long time, and especially suitable for LMA-8 with a small air-hole diameter.

The spectrometer of Agilent 86142B is used for detecting the transmission continuous broadband spectrum of light. Fig.6 shows the SPR spectrum of the PCF-SPR sensor.

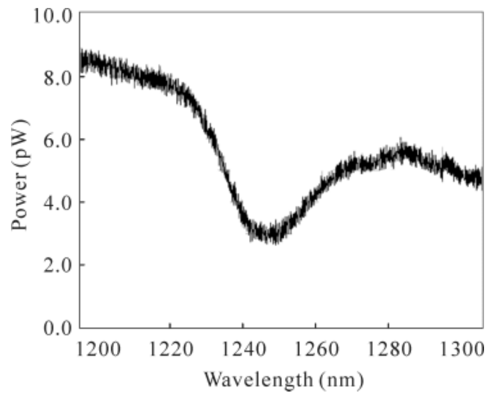

Fig.6 Transmission spectrum of the PCF-SPR sensor

It can be seen from Fig.6 that the effect of the SPR is obvious. The wave bottom of the SPR spectrum, namely the resonance wavelength, appears between 1230 nm and 1270 nm. Compared with the theoretical calculations, the offset of loss peak about 40 nm can be mainly attributed to the difference between assumption and reality about the uniformity and the thickness of the silver film. The resonance wavelength can shift when the thickness of metal film changes[6-9].

In this paper, a PCF-SPR sensor is theoretically simulated and experimentally realized. The calculations show that there is an obvious loss peak in the vicinity of 1.2 μm while the PCF of LMA-8 is selected as a sensor. The phase matching between the plasmon mode and core-guided mode is achieved, and the surface plasmon is strongly stimulated at the metal-analyte interface at this moment. The suspension of silver nanoparticle mixed with CTAB is inhaled into the PCF to form a metal film which can be stimulated to generate plasmon in the experiment. A continuous broadband light source can be realized by a bromine tungsten lamp which can be detected after PCF by a spectrometer. The experimental results verify that the loss peak shows the offset of about 40 nm. The key point of the PCF-SPR sensor is due to the metal coating. More accurate measurement depends on the uniformity and the thickness control of the metal film.

Currently, high pressure chemical deposition technique has been demonstrated to coat the uniform holes surface of a PCF with a variety of materials[14]. We believe the PCF-SPR sensor will be used in practice in the near future.

References

[1] R. Slavik, J. Homola and J. Ctyroky, Sens. Actuators B **51**, 311 (1998).

[2] J. Homola, S. S. Yee and G. Gauglitz, Sens. Actuators B **54**, 3 (1999).

[3] B. Lee, Opt. Fiber Technology **9**, 57 (2003).

[4] J. W. Xing, S. Zhu, T. Y. Wang, N. Chen and Z. Y. Chen, J. Optoelectron. Laser **22**, 693 (2011). (in Chinese)

[5] H. T. Di, Y. L. Fu and R. Q. Liu, J. Optoelectron. Laser **22**, 507 (2011). (in Chinese)

[6] A. Hassani and M. Skorobogatiy, Opt. Exp. **14**, 11616 (2006).

[7] A. Hassani and M. Skorobogatiy, J. Opt. Soc. Am. B **24**, 1423 (2007).

[8] A. K. Sharma and B. D. Gupta, Opt. Commun. **245**, 159 (2005).

[9] A. K. Sharma and B. D. Gupta, Nanotechnology **17**, 124 (2006).

[10] P. B. Johnson and R. W. Christy, Phys. Rev. B **6**, 4370 (1972).

[11] M. M. Aslan and T. Wriedt, J. Nanopart. Res. **12**, 3077 (2010).

[12] E. D. Palik, Handbook of Optical Constants of Solids, Orlando: Academic, 350 (1985).

[13] A. K. Sharma and B. D. Gupta, J. Opt. A: Pure Appl. Opt. **9**, 682 (2007).

[14] P. J. A. Sazio, A. Amezcua-Correa, C. E. Finlayson, J. R. Hayes, T. J. Scheidemantel, N. F. Baril, B. R. Jackson, D. J. Won, F. Zhang, E. R. Margine, V. Gopalan, V. H. Crespi and J. V. Badding, Science **311**, 1583 (2006).